Alzheimer's Disease Dementia Detection Using Transfer Learning Based Convolutional Neural Network Model

Amar A. Dum[1], Kshama V. Kulhalli[2], Priyanka Singh[3*]

[1]*Department of Technology, Shivaji University*
Kolhapur, Maharashtra 416004, India
E-mail: aad_tech@unishivaji.ac.in

[2]*Department of Computer Science Engineering,*
D. Y. Patil College of Engineering and Technology
Kolhapur, Maharashtra 416006, India
E-mail: kvkulhalli@gmail.com

[3]*School of Computer Science Engineering, VIT-AP University,*
Amaravati, Andhra Pradesh 522237, India.
E-mail: priyanka.cse03@gmail.com

[*]*Corresponding author*

Received: July 08, 2023 **Accepted: September 12, 2024**

Published: September 30, 2025

Abstract: *Alzheimer's disease (AD) is the most common type of dementia that is not a result of natural aging. In most countries, it is one of the leading causes of death for seniors. One of the main methods for detecting AD is by magnetic resonance imaging (MRI). Several machine learning (ML) and deep learning (DL) techniques have been put out in recent years for the automated detection of AD, but the accuracy of these techniques is currently limited. So, the primary goal of this research is to offer a model for precise AD detection that is based on transfer learning. For the purpose of detecting AD in this paper, we have used two different models. We studied and evaluated models from two different platforms, GoogleNet and residual networks (ResNet). Different variants of ResNet (ResNet18, ResNet34, ResNet50, and ResNet101) were studied. In this study, specificity, accuracy, positive predictive rate, sensitivity, F1 score, balanced accuracy, Fowlkes-Mallows index, and Youden's J statistics were investigated. ResNet18, ResNet34, ResNet50, and ResNet101 have shown a precision of 97.28%, 98.25%, 98.41%, and 98.57%. GoogleNet has accuracy rate of 96.32%. The learning curve is also presented in this work, and shows a good fit for the ResNet101 model. The proposed networks were compared on the basis of computational time. ResNet101 performed better than other networks in all the parameters and had the largest computational time. MRI images from the Alzheimer's disease neuroimaging initiative (ADNI) database have been used and compared with similar work based on ML and DL. A comparison with the existing methods showed that the proposed method could help in the reliable detection of AD.*

Keywords: *Alzheimer's disease, Dementia detection, Convolutional neural network, Transfer learning.*

Introduction

Alzheimer's disease (AD) is the most common form of dementia, affecting a patient's daily activities gradually. Most healthcare systems vastly underdiagnose dementia, owing to a lack of awareness programs and access to dementia treatment or diagnostic facilities [19]. The continuum of AD describes how the disease progresses from invisible brain changes in the affected person to brain changes that lead to memory problems and eventually physical incapacity [46]. Preclinical AD, mild cognitive impairment (MCI) AD, and Alzheimer's dementia, are the three broad phases of this continuum. As presented in Fig. 1, there are three levels of dementia associated with AD: mild, moderate, and severe. Approximately 10-17% of people with MCI eventually develop AD. However, other MCI patients stay stable years later. It is critical to identify people who are at high risk of transitioning from MCI to AD because doing so allows doctors to treat them early and use the appropriate medications to help improve patient conditions. In 2015 an estimated 5.3 million people had AD, and this number in 2050 is predicted to rise to 16 million [25].

Toward more precise AD detection, various improved imaging techniques were developed. Electroencephalogram (EEG) signals and machine learning (ML) models are one of the widely studied methods for the detection of AD [12, 32, 45]. To make a more certain prediction, various neuroimaging-based signals such as computerized tomography (CT), positron emission tomography (PET), diffusion tensor imaging, and magnetic resonance imaging (MRI) are used [4]. Because of its exceptional resolution, good contrast, and high availability in medical diagnosis, MRI is now widely used in hospitals for AD identification [50].

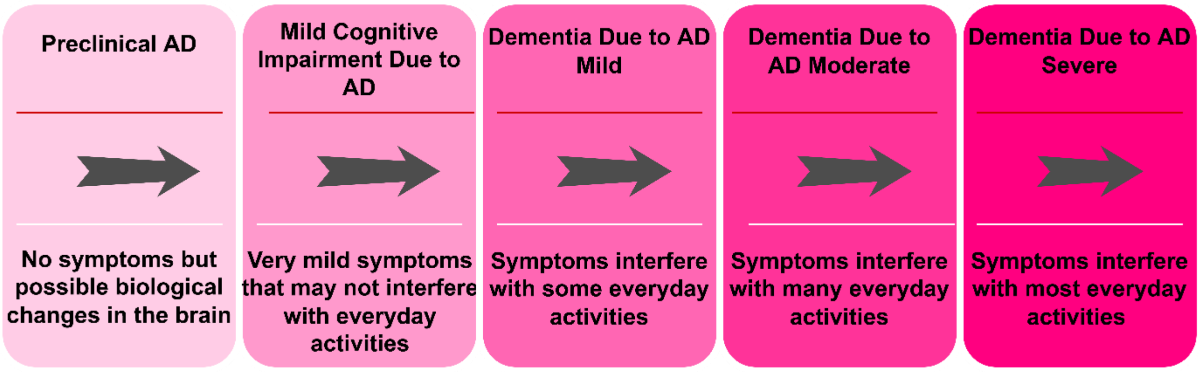

Fig. 1 Alzheimer's disease continuum

In the last decade, artificial intelligence (AI) has proven to be extremely useful in the diagnosis of AD. ML, artificial neural networks, and deep learning (DL) are the most widely used classification techniques [7, 8, 11, 14, 53]. DL has been found to be useful for large datasets, particularly image data [13, 19]. The researchers discussed DL methods for medical image analysis [35]. Although DL models are considered as "black boxes", some statistical techniques can be used to estimate the network uncertainty. Investigators conducted a survey on DL for AD [51]. It can be concluded that ML techniques are useful in determining the underlying neurological causes of brain disorders, but DL methods overcome the necessity of feature engineering [39]. The need for hand-crafted features in standard ML algorithms is a disadvantage that may result in less than ideal performance. However, DL methods are quite successful because they automatically extract significant features from the data.

The growing graphics processing unit data processing capability enabled the use of DL techniques for image classification applications [44]. [55] proposed deep transfer ensemble – an ensemble of deep neural networks (DNNs) trained with transfer learning (TL) for categorization of AD. A unique multimodal DNN with a multistage method was suggested by [37] to recognize dementia. With accuracy of 82.40%, this technique can identify who would get MCI and who will go on to develop AD three years later. For the class of people with AD, the model achieves a sensitivity of 94.23% and an accuracy of 86.30%. In order to diagnose AD, [5] suggested the convolutional neural networks (CNN) ensemble model for feature extraction and SoftMax classifier. Using left and right hippocampal regions from MRI, this model avoids overfitting and achieves an accuracy of 90.05%. [30] use a pre-trained

VGG16 model for feature extraction which uses a free surfer for preprocessing, selecting MRI slices using entropy, and classification using TL, named the mathematical model PFSECTL. The researchers achieve accuracy of 95.73%. [52] suggested a deep polynomial network that works well for small and large data sets. Using the Alzheimer's disease neuroimaging initiative (ADNI) database, the binary and multiclassification model's accuracy is 55.34%. [56] used a 3D ensemble model of CNN to present AD and MCI. Using a probability-based fusion strategy, 3D-DenseNets were optimized. Using the ADNI dataset, the model achieves classification accuracy of 97.52%. To learn AD characteristics, [21] suggested a 3D multiscale DL architecture. The system achieved a test accuracy of roughly 93.53% on subject-segregated random brain scan-partitioned dataset, with an average accuracy of 87.24%. In DL pipeline proposed by [48], the CNN model is trained using a large number of training images to perform feature categorization using scale- and shift-invariant methods. For MRI and functional magnetic resonance imaging (fMRI), the model achieves accuracy of 94.32% and 97.88%, respectively.

DL models have been successfully used to analysis neuroimages from MRIs [33]. On the other hand, TL has gained popularity, which enables DL training to be effective in situations of insufficient data [29]. TL is suggested when compared with human behavior, can be applied to solve new, challenging situations. In this work, TL models – GoogleNet and residual networks (ResNet) were studied for the detection of AD. ResNet architecture offers several significant advantages, particularly in the training of very DNNs. One of its key strengths is the mitigation of the problem of vanishing gradients, which often hampers the training of deep networks [26]. By introducing skip connections, ResNet allows gradients to flow more effectively during backpropagation, ensuring that the network can learn even when it becomes very deep. This design also addresses the degradation problem, where adding more layers might otherwise lead to worse performance, by ensuring that additional layers contribute positively or at least do no harm. Consequently, ResNet enables the training of deeper networks, such as ResNet18, ResNet34, ResNet50, and ResNet101, which are capable of learning complex feature hierarchies, resulting in improved accuracy on tasks like image classification, object detection, and segmentation. Moreover, the architecture simplifies the optimization process, leading to smoother and more reliable training, and is known for its flexibility and generalization across different tasks and domains [49]. ResNet's success on benchmark datasets like ImageNet has made it a popular choice for TL, where pre-trained ResNet models serve as powerful starting points for fine tuning on specific tasks with smaller datasets. Overall, ResNet's ability to overcome common DL challenges, achieve high accuracy, and adapt to various applications makes it a highly effective and versatile architecture in the field of computer vision [27, 60]. The capability of ResNet has been comprehensively studied in this work for the detection of AD. A description and analysis are presented below.

Materials and methods

Database description

This study dealt with AD identification used data from ADNI database [61] – the private-public partnership in USA and Canada introduced in 2004. The primary aim of ADNI dataset has been image analysis, including MRI, PET, and various clinical, neuropsychological, and biological markers. In this work, MRIs from this database have been used for the detection of AD.

Proposed methodology

The methodology is represented graphically in Fig. 2.

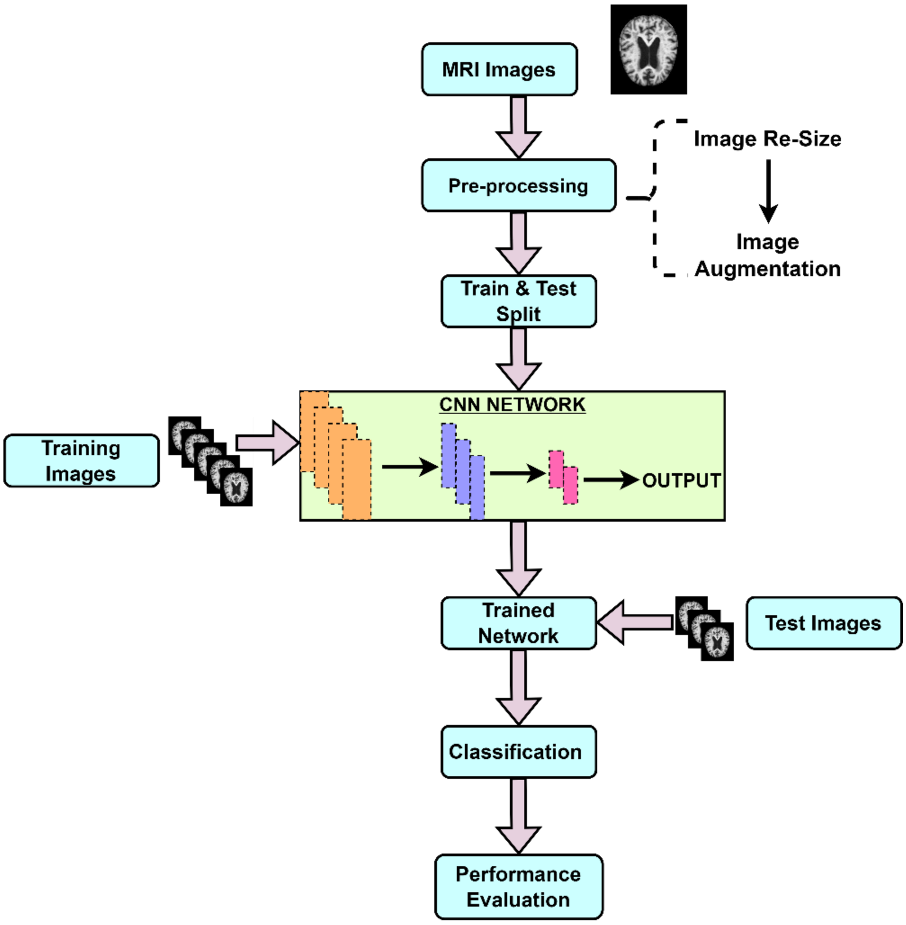

Fig. 2 Alzheimer's disease detection flow diagram

Pre-processing

The pre-processing was done to the images before their application to the CNN network. All images were resized in a manner that accommodates to the input size of the respective CNN. We created "augmented image database" from these resized images. The image augmentation techniques used in this work are rotation, reflection, translation, scaling, and shearing. Example with original image and the augmented images are shown in Fig. 3.

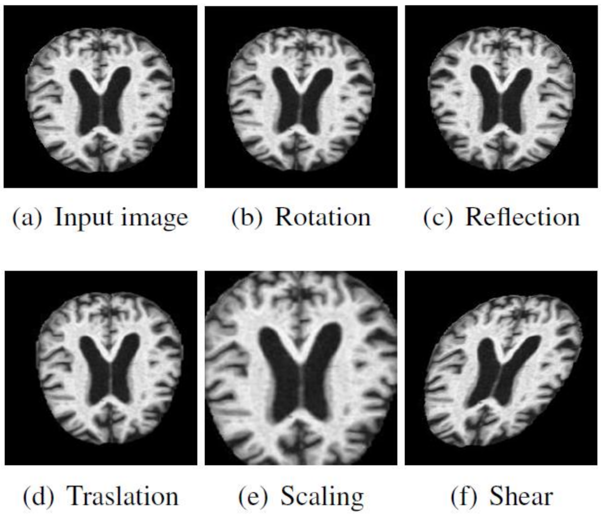

Fig. 3 Augmented images of Alzheimer's dataset

Convolutional neural network

CNNs are currently widely used for applications in AI, medical image processing, and image classification [29, 31]. CNN offers better results for larger datasets. In this work, for the purpose of detecting AD, we employed ResNet and GoogleNet. The fundamental architecture of CNN consists of several key components: convolutional layers, pooling layers, and fully connected layers. Each component plays a specific role in extracting features, reducing dimensionality, and making predictions.

Convolutional layers are composed of a rectangular grid of neurons. A rectangular grid of neurons must also exist in the layer above. Each neuron in this layer gets input from a layer above it, and all of the neurons in this layer have the same section weights. Since the weights determine a convolutional filter, this layer is just a convolution of the output of the layer before. The convolutional layer applies a set of filters (or kernels) to the input image or feature map. The output of the convolution operation is a feature map:

$$F_{i,j}^{k} = \sum_{m=1}^{M} \sum_{n=1}^{N} I_{i+m-1,j+n-1} . k_{m,n}^{k} + b_k, \tag{1}$$

where $F_{i,j}^{k}$ is the resulting feature map after applying the k-th filter; $I_{i+m-1,j+n-1}$ is the input image or feature map, i and j are the spatial dimensions of the output feature map; $k_{m,n}^{k}$ is the k-th filter with dimensions $m \times n$; and b_k is the bias term for the k-th filter.

After that, the convolutional layer's non-linearity is used. Next, the non-linearity of the convolutional layer is employed:

$$A_{i,j}^{k} = ReLU\left(F_{i,j}^{k}\right) = \max(0, F_{i,j}^{k}), \tag{2}$$

where $A_{i,j}^{k}$ is the activation after applying the rectified linear unit (ReLU) function on the feature map.

The ReLU is responsible for introducing these non-linarites. In comparison to other functions, this ReLU function performs well. The feature map which is produced by the convolutional layer and the ReLU function, maps the input data. After the convolutional layer, the data are processed in the pooling layer.

Pooling layers reduce the number of parameters when the images are too large. Spatial pooling, sometimes referred to as "down-sampling", reduces the dimensionality of each map while retaining essential data. There are three basic types of pooling layers. The maximum pooling layers are straight-forward and use the highest value for the ReLU mapped element. The average pooling layer takes the average of its input values. The sum-pooling layer is the total of all elements on the map. This work uses average pooling layer.

$$P_{i,j}^{k} = \frac{1}{mxn} \sum_{p=0}^{m-1} \sum_{q=1}^{n-1} A_{i+p,j+q}, \tag{3}$$

where $P_{i,j}^{k}$ is the pooled feature map, over a window of size $m \times n$ in the feature map A.

Fully connected layer converts the input from the convolutional and pooling layers from the preceding layers into vectors. The detection of AD is done by using the sigmoid during binary and SoftMax activation function for multiclass classification. The CNN first must be trained using training parameters before it can classify the processed data. We used the adaptive moment estimation (Adam) optimizer [1] because it updates CNN network weights based on the training data. Adam optimizer is an extension of the stochastic gradient descent optimization method which gained popularity due to its adaptive learning rate and the ability to handle sparse gradients and noisy problems [1]. The involved steps are formulated as follows:

Step 1. Initialization: Initialize the parameters θ_θ, m_0, and v_0.

Step 2. Update biased first moment estimate: This computes a running average of the gradients, which is biased toward the initial values of the gradients.

$$m_t = \beta_1 m_{t-1} + (1 - \beta_1) g_t \tag{4}$$

Step 3. Update biased second-moment estimate: This computes a running average of the squared gradients.

$$v_t = \beta_2 v_{t-1} + (1 - \beta_2) g_t^2 \tag{5}$$

Step 4. Compute bias-corrected first moment estimate: This step corrects the bias introduced by initializing $m_0 = 0$.

$$\hat{m}_t = \frac{m_t}{1-\beta_1^t} \tag{6}$$

Step 5. Compute bias-corrected second moment estimate: This step corrects the bias introduced by initializing $v_0 = 0$.

$$\hat{v}_t = \frac{v_t}{1-\beta_2^t} \tag{7}$$

Step 6. Update parameters: This is the actual update rule for the parameters, where α is the learning rate, and ε is a small number to prevent division by zero.

$$\theta_{t+1} = \theta_t - \alpha \frac{\hat{m}_t}{\sqrt{\hat{v}_t}+\varepsilon} \tag{8}$$

Adam adapts the learning rate for each parameter individually based on the estimates of the first and second moments, leading to better performance on problems with sparse gradients [47]. Adam is invariant to rescaling of the gradient, making it robust to different types of data and model structures. After training Adam CNN, testing and classification of MRI have to be done. For classification, we used five CNN networks: GoogleNet, ResNet18, ResNet34, ResNet50, and ResNet101. ResNet is a type of DNN architecture that has been shown to give good results in a wide range of computer vision tasks, such as image classification, object detection, and semantic segmentation [26].

Residual networks

In ResNet the issue of vanishing gradients in DNNs is addressed by [26]. When a network's depth increases, it becomes more challenging to train because the gradients may get incredibly small, making it more challenging to update the network's weights during backpropagation. The skip connection, known as a shortcut link, introduced by ResNet, enables the gradient to flow straight from older layers to subsequent layers. This allows ResNet to train much deeper networks which can result in better accuracy than other architectures [26]. A building block for residual based learning with skip connection is shown in Fig. 4.

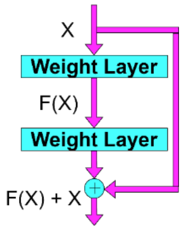

Fig. 4 Skip connections in ResNet

ResNet also has the benefit of learning more intricate and complex feature representations by stacking multiple residual blocks. The skip connection enables the network to learn residual features which capture the difference between the input and output of the block [49]. Each residual block is made up of two or more convolutional layers. When performing tasks, like image classification, where fine-grained distinctions are crucial, this help network to learn more precise and nuanced representations of the input data. ResNet is highly effective in classification tasks due to several key innovations that address challenges faced by DNNs, especially the degradation problem [27, 60].

As the depth of a neural network increases, it becomes difficult to train due to issues like vanishing gradients and degradation of performance. ResNet introduces residual blocks which allow the network to learn residuals (the difference between the desired output and the actual output of a block). This is done by adding a shortcut or skip connection that bypasses one or more layers. This helps the network focus on learning the residual mapping rather than the full transformation, making it easier to optimize.

The skip connections allow gradients to flow directly through the network, bypassing intermediate layers. This mitigates the vanishing gradient problem, enabling the effective training of very deep networks. Instead of learning a complicated transformation, the network learns simpler residuals which are more efficient. The skip connections ensure that at the very least, the network can copy the input if the deeper layers do not learn anything useful which avoids performance degradation.

ResNet enables the construction of extremely deep networks (e.g. ResNet18, ResNet34, ResNet50, ResNet101) while maintaining or improving performance. Deep networks can capture more complex patterns and features contributing to better classification results. The architectural design of ResNet with its residual blocks helps prevent overfitting even when trained on large datasets. The residual connections act as regularizes, ensuring the network generalizes well to unseen data.

Results

A variety of metrics can be used to assess classification. The following performance metrics are the most frequently employed for classification problems: sensitivity (Se), specificity (Sp), positive predictive rate (PPR), accuracy (Acc), F1 score (F1), balanced accuracy (BAcc), Fowlkes-Mallows index (FMI), and Youden's J statistic (J-Stat). These are collectively referred to as a system's performance metrics and are used in this study. Mathematically, Sp and Se show how accurately a test can detect the existence or absence of a condition. Instances of AD detection are regarded as "positive" while normal conditions are regarded as "negative". PPR stands for the percentage of positive outcomes from diagnostic tests and statistics that are actually genuine positives. The accuracy of a set of measurements refers to the degree to which they match the true value. The accuracy of a test is measured by the F1. Confusion matrices are measured using FMI, an external evaluation technique. A dichotomous diagnostic test's performance is summarized by the J-Stat statistic. All their performance metrics are evaluated as follows:

$$Se = \frac{TP}{TP+FN}; \quad (9)$$

$$Sp = \frac{TN}{TN+FP}; \quad (10)$$

$$PPR = \frac{TP}{TP+FP}; \quad (11)$$

$$Acc = \frac{TP+TN}{TP+TN+FP+FN}; \quad (12)$$

$$F1 = \frac{2\times TP}{2\times TP+FP+FN}; \quad (13)$$

$$BAcc = \frac{Se+Sp}{2}; \quad (14)$$

$$FMI = \sqrt{Se \times PPR}; \quad (15)$$

$$J\ stat = Se + Sp - 1; \quad (16)$$

where true positive (*TP*) is the number of positive predictions made when positive labels are actually present; false positive (*FP*) is the number of positive predictions made when negative labels are actually present; true negative (*TN*) is the number of negative predictions made when negative labels are actually present; false negative (*FN*) is the number of negative predictions made when positive labels are actually present.

For comparison, we used the GoogleNet and ResNet models of DNNs. When compared to GoogleNet model, it was shown that the ResNet model performs incredibly well. Four different variants of ResNet architectures (ResNet18, ResNet34, ResNet50, and ResNet101) were compared. The results are presented in Table 1. GoogleNet achieved Acc of 96.32%, Se of 95.73%, and Sp of 96.88%. ResNet18, ResNet34, ResNet50, ResNet101 gave Acc of 97.28%, 98.25%, 98.41%, and 98.57%, respectively. ResNet101 has given Se, Sp, PPR, Acc, F1, BAcc, FMI, and J-Stat of 98.05%, 99.06%, 99.00%, 98.57%, 98.52%, 98.55%, 98.52%, and 97.11%, respectively.

Table 1. Comparative results for ResNet and GoogleNet model

Model	Se	Sp	PPR	Acc	F1	BAcc	FMI	J-Stat
GoogleNet	0.9573	0.9688	0.9666	0.9632	0.9619	0.963	0.9619	0.9260
ResNet18	0.9606	0.9844	0.9831	0.9728	0.9717	0.9725	0.9718	0.9450
ResNet34	0.9771	0.9875	0.9866	0.9825	0.9819	0.9823	0.9819	0.9646
ResNet50	0.9788	0.9891	0.9883	0.9841	0.9835	0.9839	0.9835	0.9679
ResNet101	0.9805	0.9906	0.9900	**0.9857**	0.9852	0.9855	0.9852	0.9711

The receiver operating characteristic (ROC) curve is a graph that shows how well classification model performs at each level of classification. Two parameters are represented in this curve: the false positive rate (FPR) and the true positive rate (TPR). TPR vs. FPR are plotted on ROC curve at various categorization criteria. More items are classified as positive when the classification threshold is lowered which raises the number of both false positives and true positives. The ROC curve of ResNet101 model is shown in Fig. 5. For algorithms that learn (optimize their internal parameters) gradually over time, like DL neural networks, learning curves are frequently employed in machine learning. There are three typical observations that can be made in learning curves: over fit, under fit, and good fit. A learning plot of under fit model has the following characteristics: regardless of training, the training loss is constant; until the training is over, the training loss keeps getting smaller.

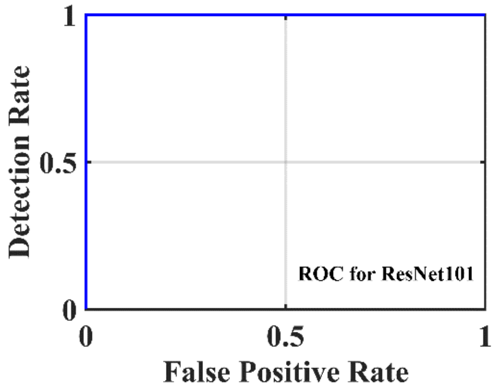

Fig. 5 ROC curve for ResNet101

A learning plot of over fit model has the following characteristics: with learning, the plot of training loss keeps declining; a point is reached where the validation loss plot starts to increase once more.

A learning plot of a good fit model has the following characteristics: the training loss plot declines until it reaches a stable position; the training loss and validation loss are closely separated on the plot of validation loss as it decreases to a stable point.

The learning plot of the proposed model is a good fit as it satisfies the criterion of good fit in machine learning. Comparing only the metrics discussed in Eqs. (9)-(16) is not fair because different CNN models have different levels of complexity (number of layers), and their accuracy and computation time is dependent on that. GoogleNet is the quickest because it has 22 layers, whereas ResNet101 is a CNN with 101 layers, so it took more time.

Discussion

In this study, a method for correctly identifying dementia using brain MRI is provided. The extraction of features use the segmentation based fractal texture analysis (SFTA) method. The binary images produced by the two threshold binary decomposition technique once the image has been broken down are used to extract fractal dimensions and texture properties. The classification of dementia is carried out using neural networks. With a classification accuracy of 97.50%, this technique has been successfully tested using 3D brain MRI from the OASIS dataset.

[6] proposed a neural network based method. [20] offered a deep belief network (DBN) based classification strategy for AD based on structural modalities and has strength in terms of prediction models. Support vector machines (SVM) have been contrasted with DBN in classification models. The outcome demonstrates that this strategy performs SVM and the present method in the earlier investigation. The Acc, Se, and Sp of the DBN are 91.76%, 90.59%, and 92.96%, respectively. In order to minimize the dimensionality of extracted features from MRI, a novel feature abstraction method using a sparse autoencoder is proposed in [9, 10].

Then, in order to assess the prediction accuracy (PCA) of a linear discriminant analysis (LDA) and a logistic regression classifier, these features and those derived via the well-known PCA approach are utilized to train the respective classifiers. The experimental results demonstrate that the proposed approach produces a classification accuracy that is 8.00% greater than that of the PCA. For the long-term examination of structural MRI in AD diagnosis, [16] provide classification framework based on a combination of convolutional and recurrent neural networks (RNN). In order to learn the spatial properties of MRI for the classification task, CNN are first built. In order to extract the longitudinal features for AD classification, RNN with cascading three bidirectional gated recurrent units (BGRU) layers are then built on the CNN outputs at various time points. According to experimental findings, the suggested technique obtains classification accuracy of 91.33%. To provide a quantitative index of pattern matching for the prediction of the transition from MCI to AD, a novel data mining framework was designed and combined with three different classifiers, including SVM, Bayes statistics, and voting feature intervals [43]. By using feature selection methods, the brain regions with the highest accuracy for differentiating between AD and MCI were found, with accuracy of 92.00%. Multifold Bayesian kernelization (MBK) is a novel diagnosis approach that suggest models for diagnosis process as a synthesis analysis of multi-modal biomarkers [36]. Each biomarker is given a kernel using MBK that maximizes the local neighborhood affinity, and each biomarker's contribution is then assessed using a Bayesian framework. By combining the output diagnosis probabilities of several biomarkers, MBK implements a novel diagnosis scheme that might determine the subject's diagnosis. [41] proposed a technique based on the lattice computing (LC) scheme for AD detection using MRI data. A kernel nearest neighbors (k-NN) classifier in the LC context pursues computer assisted diagnostics by approaching this task from two separate angles. In order to classify the subjects inside the lattice space, it first conducts dimensionality reduction over the high dimensional feature vectors. In order to diagnose and predict MCI and AD, a unique framework that integrates the two conceptually dissimilar techniques of sparse regression and DL is put [54]. To be more precise, at first train numerous sparse regression models with a different value for a regularization control parameter. [17] uses unique texture and other related variables taken from structural MRI to propose a multiclass DL classification of AD. Using data augmentation for 3D MRI views from the OASIS dataset, [3] used TL based approach. While employing a single MRI, the suggested model's accuracy is 98.41%, and when using 3D views, accuracy is 95.11%. From structural MRI to diffusion tensor imaging, [2] suggest a method of cross-modal TL. To train on mean diffusivity data, models that have already been trained on a structural MRI dataset with domain-dependent data augmentation are used as the initialization of the network parameters. The technique reduces the over fitting phenomenon, enhances learning efficiency, and hence boost prediction accuracy. The canonical representation of brain areas is made possible by the method [22], which use statistical learning and a feature space made up of projection based shape descriptors. The structures most severely impacted by the disease are automatically identified. A novel multi-domain transfers learning architecture is proposed for the combined learning of tasks in several auxiliary domains and the target domain [15]. [38] proposed the use of 3D MRI for AD stages classification and detection using TL. The ability to diagnose AD through the fusion of multimodal neuroimaging data has been demonstrated using techniques like PET and MRI [52]. A deep 3D CNN that can learn generic features capturing AD biomarkers and distinguish between Alzheimer's brain and a normal healthy brain based on brain MRI has been proposed to predict AD [42]. [40] examine how DL architectures can be used to build classification methods that are applied to the parts of the brain identified by the automated anatomical labeling (AAL). The AAL atlas areas have been used to divide grey matter pictures from each brain region into 3D patches, and these patches are used to train various deep belief networks. Based on MRI and PET, a comprehensive DL system may be used to determine the various stages of AD progression. By eliminating weight coadaptation, a common source of overfitting in DL, [34] used the dropout strategy to enhance traditional DL. Additionally, [34] added a multitask learning technique, an adjustable learning factor, and stability selection to the DL framework. [37] suggest a unique DL framework that uses a multimodal and multiscale DNN to distinguish between people with AD. This approach has an accuracy of 82.40% for detecting people with MCI.

As presented in Table 2, the proposed model outperforms the existing state-of-the-art method based on ML or DL.

Table 2. Comparison of the proposed model with existing methods for AD detection

	Ref. №	**Method**	**Imaging technique**	**Accuracy, [%]**
Machine learning based approach	[6]	Feedforward neural network	MRI	97.50
	[20]	DBN	MRI	91.70
	[9, 10]	CNN + logistic regression	MRI	74.93
	[16]	RNN	MRI	89.70
	[23]	CNN	MRI	96.00
	[28]	Partial least squares regression + k-NN	SPECT images	88.00
	[43]	Data mining + SVM	MRI	90.00
	[36]	Multifold bayesian	MRI	84.74
	[41]	LC + k-NN	MRI	80.00
	[59]	CNN	MRI	92.06
	[54]	Deep ensemble sparse regression network	MRI	90.28
	[17]	Stacked auto-encoder + DNN	MRI	56.00
Deep learning based approach	[3]	TL	MRI	98.41
	[2]	TL	MRI	92.50
	[58]	TL	MRI	90.60
	[22]	TL	MRI	83.50
	[18]	TL	MRI	83.00
	[15]	TL	MRI	94.70
	[38]	TL	MRI	92.85
	[52]	Multi-modal stacked deep polynomial networks + SVM	MRI, PET	97.13
	[42]	Sparse autoencoder + 3D CNN	MRI	95.39
	[40]	AAL + SVM	MRI, PET	90.00
	[57]	2D CNN	MRI	97.65
	[34]	Stacked robust deep model (RBM) + SVM	MRI, PET, CSF	91.40
	[24]	Sparse autoencoder + CNN	MRI	94.74
	[37]	Multimodal and multiscale DNN	MRI, PET	84.60
	[54]	Sparse regression models + 2D CNN	MRI	91.02
	Proposed method	**TL**	**MRI**	**98.57**

The proposed method has performed better compared with ML based models [6, 28, 36, 41, 43]. DL models have an advantage over ML models which do not require feature engineering. The proposed method has performed significantly better compared to DL based models [9, 10, 16, 17, 20, 23, 37, 42, 57, 59]. The proposed method also performs better compared with models based on DL in their feature extraction stage and ML in the classification stage [28, 40, 41, 43, 52]. The proposed method performed admirably better compared to TL methods [2, 3, 15, 18, 22, 38, 58]. Improved accuracy in this method could help in more reliable detection of AD.

Conclusions

This paper presents a technique to detect AD using TL models. GoogleNet and ResNet models have been studied. ResNet performed significantly better in all parameters (Se, Sp, PPR, Acc, F1, BAcc, FMI, and J-Stat) studied in this work. Four different variants of ResNet were studied, and ResNet101 performed the best among them. This study also presents a computational analysis of these models in terms of execution time. It was observed that GoogleNet was the fastest among the studied models, and ResNet101 took the longest time to execute but achieved the highest accuracy. Analysis of the learning curve showed that the selected model was a good fit. MRI from the ADMI database were used in this work for the training and validation of the proposed models. Compared to the existing state-of-the-art methods, the proposed technique has admirable performance, so it can be a reliable approach for Alzheimer's disease detection.

References

1. Adam K. D. B. J. (2014). A Method for Stochastic Optimization, arXiv, 1412(6), 6980.
2. Aderghal K., A. Khvostikov, A. Krylov, J. Benois-Pineau, et al. (2018). Classification of Alzheimer Disease on Imaging Modalities with Deep CNNs Using Cross-modal Transfer Learning, 31st International Symposium on Computer-based Medical Systems, 345-350.
3. Afzal S., M. Maqsood, F. Nazir, U. Khan, et al. (2019). A Data Augmentation-based Framework To Handle Class Imbalance Problem for Alzheimer's Stage Detection, IEEE Access, 7, 115528-115539.
4. Afzal S., M. Maqsood, U. Khan, I. Mehmood, et al. (2021). Alzheimer Disease Detection Techniques and Methods: A Review, International Journal of Interactive Multimedia and Artificial Intelligence, 6(7), 26-38.
5. Ahmed S., K. Y. Choi, J. J. Lee, B. C. Kim, et al. (2019). Ensembles of Patch-based Classifiers for Diagnosis of Alzheimer Diseases, IEEE Access, 7, 73373-73383.
6. Akhila J., C. Markose, R. Aneesh (2017). Feature Extraction and Classification of Dementia with Neural Network, International Conference on Intelligent Computing, Instrumentation and Control Technologies, 1446-1450.
7. Alam S., G. R. Kwon, Alzheimer's Disease Neuroimaging Initiative (2017). Alzheimer Disease Classification Using KPCA, LDA, and Multi-kernel Learning SVM, International Journal of Imaging Systems and Technology, 27(2), 133-143.
8. Alam S., G. R. Kwon, J. I. Kim, C. S. Park (2017). Twin SVM-based Classification of Alzheimer's Disease Using Complex Dual-tree Wavelet Principal Coefficients and LDA, Journal of Healthcare Engineering, 2017(1), 8750506.
9. Alkabawi E. M., A. R. Hilal, O. A. Basir (2017). Computer-aided Classification of Multi-types of Dementia via Convolutional Neural Networks, 2017 IEEE International Symposium on Medical Measurements and Applications, 45-50.
10. Alkabawi E. M., A. R. Hilal, O. A. Basir (2017). Feature Abstraction for Early Detection of Multi-type of Dementia with Sparse Auto-encoder, 2017 IEEE International Conference on Systems, Man, and Cybernetics (SMC), 3471-3476.

11. Al-Naami B., N. Gharaibeh, A. A. Kheshman (2013). Automated Detection of Alzheimer Disease Using Region Growing Technique and Artificial Neural Network, World Academy of Science, Engineering and Technology, International Journal of Biomedical and Biological Engineering, 7(5), 204-208.
12. Bairagi V. (2018). EEG Signal Analysis for Early Diagnosis of Alzheimer Disease Using Spectral and Wavelet-based Features, International Journal of Information Technology, 10(3), 403-412.
13. Basaia S., F. Agosta, L. Wagner, E. Canu, et al. (2019). Automated Classification of Alzheimer's Disease and Mild Cognitive Impairment Using a Single MRI and Deep Neural Networks, NeuroImage: Clinical, 21, 101645.
14. Chaplot S., L. M. Patnaik, N. R. Jagannathan (2006). Classification of Magnetic Resonance Brain Images Using Wavelets as Input to Support Vector Machine and Neural Network, Biomedical Signal Processing and Control, 1(1), 86-92.
15. Cheng B., M. Liu, D. Shen, Z. Li, et al. (2017). Multi-domain Transfer Learning for Early Diagnosis of Alzheimer's Disease, Neuroinformatics, 15(2), 115-132.
16. Cui R., M. Liu, G. Li (2018). Longitudinal Analysis for Alzheimer's Disease Diagnosis Using RNN, 15th International Symposium on Biomedical Imaging, 1398-1401.
17. Dolph C. V., M. Alam, Z. Shboul, M. D. Samad, et al. (2017). Deep Learning of Texture and Structural Features for Multiclass Alzheimer's Disease Classification, International Joint Conference on Neural Networks, 2259-2266.
18. Dyrba M., M. Ewers, M. Wegrzyn, I. Kilimann, et al. (2013). Robust Automated Detection of Microstructural White Matter Degeneration in Alzheimer's Disease Using Machine Learning Classification of Multicenter DTI Data, PloS One, 8(5), e64925.
19. Ebrahimighahnavieh M., S. Luo, R. Chiong (2020). Deep Learning to Detect Alzheimer's Disease from Neuroimaging: A Systematic Literature Review, Computer Methods and Programs in Biomedicine, 187, 105242.
20. Faturrahman M., I. Wasito, N. Hanifah, R. Mufidah (2017). Structural MRI Classification for Alzheimer's Disease Detection Using Deep Belief Network, 11th International Conference on Information & Communication Technology and System, 37-42.
21. Ge C., Q. Qu, I. Y. H. Gu, A. S. Jakola (2019). Multiscale Deep Convolutional Networks for Characterization and Detection of Alzheimer's Disease Using MR Images, IEEE International Conference on Image Processing, 789-793.
22. Glozman T., J. Solomon, F. Pestilli, L. Guibas, et al. (2017). Shape-attributes of Brain Structures as Biomarkers for Alzheimer's Disease, Journal of Alzheimer's Disease, 56(1), 287-295.
23. Gunawardena K., R. Rajapakse, N. Kodikara (2017). Applying Convolutional Neural Networks for Pre-detection of Alzheimer's Disease from Structural MRI Data, 24th International Conference on Mechatronics and Machine Vision in Practice, 1-7.
24. Gupta A., M. Ayhan, A. Maida (2013). Natural Image Bases to Represent Neuroimaging Data, International Conference on Machine Learning, 987-994.
25. Hazarika R. A., A. K. Maji, S. N. Sur, B. S. Paul, et al. (2021). A Survey on Classification Algorithms of Brain Images in Alzheimer's Disease Based on Feature Extraction Techniques, IEEE Access, 9, 58503-58536.
26. He K., X. Zhang, S. Ren, J. Sun (2016). Deep Residual Learning for Image Recognition, IEEE Conference on Computer Vision and Pattern Recognition, 770-778.
27. He K., X. Zhang, S. Ren, J. Sun (2016). Identity Mappings in Deep Residual Networks, European Conference on Computer Vision, 630-645.
28. Horn J. F., M. O. Habert, A. Kas, Z. Malek, et al. (2009). Differential Automatic Diagnosis between Alzheimer's Disease and Frontotemporal Dementia Based on Perfusion SPECT Images, Artificial Intelligence in Medicine, 47(2), 147-158.

29. Jadhav S. B., V. R. Udupi, S. B. Patil (2021). Identification of Plant Diseases Using Convolutional Neural Networks, International Journal of Information Technology, 13(6), 2461-2470.
30. Jain R., N. Jain, A. Aggarwal, D. J. Hemanth (2019). Convolutional Neural Network-based Alzheimer's Disease Classification from Magnetic Resonance Brain Images, Cognitive Systems Research, 57, 147-159.
31. Kalaiselvi T., S. Padmapriya, P. Sriramakrishnan, K. Somasundaram (2020). Deriving Tumor Detection Models Using Convolutional Neural Networks from MRI of Human Brain Scans, International Journal of Information Technology, 12, 403-408.
32. Kulkarni N. (2018). Use of Complexity-based Features in Diagnosis of Mild Alzheimer Disease Using EEG Signals, International Journal of Information Technology, 10(1), 59-64.
33. LeCun Y., Y. Bengio, G. Hinton (2015). Deep Learning, Nature, 521(7553), 436-444.
34. Li F., L. Tran, K. H. Thung, S. Ji, et al. (2015). A Robust Deep Model for Improved Classification of AD/MCI Patients, IEEE Journal of Biomedical and Health Informatics, 19(5), 1610-1616.
35. Litjens G., T. Kooi, B. E. Bejnordi, A. A. A. Setio, et al. (2017). A Survey on Deep Learning in Medical Image Analysis, Medical Image Analysis, 42, 60-88.
36. Liu S., Y. Song, W. Cai, S. Pujol, et al. (2013). Multifold Bayesian Kernelization in Alzheimer's Diagnosis, International Conference on Medical Image Computing and Computer-assisted Intervention, 303-310.
37. Lu D., K. Popuri, G. W. Ding, R. Balachandar, et al. (2018). Multimodal and Multiscale Deep Neural Networks for the Early Diagnosis of Alzheimer's Disease Using Structural MR and FDG-PET Images, Scientific Reports, 8(1), 1-13.
38. Maqsood M., F. Nazir, U. Khan, F. Aadil, et al. (2019). Transfer Learning Assisted Classification and Detection of Alzheimer's Disease Stages Using 3D MRI Scans, Sensors, 19(11), 2645.
39. Mateos-Pérez J. M., M. Dadar, M. Lacalle-Aurioles, Y. Iturria-Medina, et al. (2018). Structural Neuroimaging as Clinical Predictor: A Review of Machine Learning Applications, NeuroImage: Clinical, 20, 506-522.
40. Ortiz A., J. Munilla, J. M. Gorriz, J. Ramirez (2016). Ensembles of Deep Learning Architectures for the Early Diagnosis of the Alzheimer's Disease, International Journal of Neural Systems, 26(07), 1650025.
41. Papakostas G. A., A. Savio, M. Graña, V. G. Kaburlasos (2015). A Lattice Computing Approach to Alzheimer's Disease Computer-assisted Diagnosis Based on MRI Data, Neurocomputing, 150, 37-42.
42. Payan A., G. Montana (2015). Predicting Alzheimer's Disease: A Neuroimaging Study with 3D Convolutional Neural Networks, arXiv, 1502, 02506.
43. Plant C., S. J. Teipel, A. Oswald, C. Böhm, et al. (2010). Automated Detection of Brain Atrophy Patterns Based on MRI for the Prediction of Alzheimer's Disease, Neuroimage, 50(1), 162-174.
44. Plis S. M., D. R. Hjelm, R. Salakhutdinov, E. A. Allen, et al. (2014). Deep Learning for Neuroimaging: A Validation Study, Frontiers in Neuroscience, 8, 229.
45. Putri F. D., V. Nadhira (2023). Quantitative EEG Based on Direct Recording and Source Localization Estimation in Repetitive Hand Motor Activity, International Journal Bioautomation, 27(1), 51.
46. Rath S. N., M. Patri (2020). Understanding miRNA Based Gene Regulation in Parkinson's Disease: An *in silico* Approach, International Journal Bioautomation, 24(1).
47. Ruder S. (2016). An Overview of Gradient Descent Optimization Algorithms, arXiv, 1609, 04747.

48. Sarraf S., D. D. DeSouza, J. Anderson, G. Tofighi, et al. (2016). DeepAD: Alzheimer's Disease Classification via Deep Convolutional Neural Networks Using MRI and fMRI, BioRxiv, 070441.
49. Shafiq M., Z. Gu (2022). Deep Residual Learning for Image Recognition: A Survey, Applied Sciences, 12(18), 8972.
50. Shaikh T. A., R. Ali (2022). Enhanced Computerized Diagnosis of Alzheimer's Disease from Brain MRI Images Using a Classifier Merger Strategy, International Journal of Information Technology, 1-13.
51. Shen D., G. Wu, H. I. Suk (2017). Deep Learning in Medical Image Analysis, Annual Review of Biomedical Engineering, 19, 221.
52. Shi J., X. Zheng, Y. Li, Q. Zhang, et al. (2017). Multimodal Neuroimaging Feature Learning with Multimodal Stacked Deep Polynomial Networks for Diagnosis of Alzheimer's Disease, Journal of Biomedical and Health Informatics, 22(1), 173-183.
53. Singh R. S., D. J. Gelmecha, S. Mishra, G. Dengia, et al. (2022). A Novel Machine Learning Approach for Detection of Coronary Artery Disease Using Reduced Nonlinear and Chaos Features, International Journal Bioautomation, 26(3).
54. Suk H. I., S. W. Lee, D. Shen, A. D. N. Initiative (2017). Deep Ensemble Learning of Sparse Regression Models for Brain Disease Diagnosis, Medical Image Analysis, 37, 101-113.
55. Tanveer M., A. H. Rashid, M. Ganaie, M. Reza, et al. (2021). Classification of Alzheimer's Disease Using Ensemble of Deep Neural Networks Trained through Transfer Learning, Journal of Biomedical and Health Informatics, 26(4), 1453-1463.
56. Wang H., Y. Shen, S. Wang, T. Xiao, et al. (2019). Ensemble of 3D Densely Connected Convolutional Network for Diagnosis of Mild Cognitive Impairment and Alzheimer's Disease, Neurocomputing, 333, 145-156.
57. Wang S. H., P. Phillips, Y. Sui, B. Liu, et al. (2018). Classification of Alzheimer's Disease Based on Eight-layer Convolutional Neural Network with Leaky Rectified Linear Unit and Max Pooling, Journal of Medical Systems, 42(5), 1-11.
58. Wang S., Y. Shen, W. Chen, T. Xiao, et al. (2017). Automatic Recognition of Mild Cognitive Impairment from MRI Images Using Expedited Convolutional Neural Networks, International Conference on Artificial Neural Networks, 373-380.
59. Wang Y., Y. Yang, X. Guo, C. Ye, et al. (2018). A Novel Multimodal MRI Analysis for Alzheimer's Disease Based on Convolutional Neural Network, 40th Annual International Conference of the IEEE Engineering in Medicine and Biology Society, 754-757.
60. Zhang C., S. Bengio, M. Hardt, B. Recht, et al. (2021). Understanding Deep Learning (Still) Requires Rethinking Generalization, Communications of the ACM, 64(3), 107-115.
61. https://adni.loni.usc.edu/ (Access data 28 July 2025).

Amar A. Dum, Ph.D. Student
E-mail: aad_tech@unishivaji.ac.in

Amar Dum is currently a Ph.D. Student in the Department of Electronics Engineering at Shivaji University, Kolhapur, India. He earned his B.Sc. Technical Degree in Electronics and Telecommunication Engineering in 2007 and M.Sc. Technical Degree in Electronics Technology in 2010, both from Shivaji University, Kolhapur, India. His current research focuses on image analysis, machine learning, and deep learning. As a dedicated scholar, he is contributing to advancements in these areas through his doctoral studies at Shivaji University, India.

Prof. Kshama V. Kulhalli, Ph.D.
E-mail: kvkulhalli@gmail.com

Prof. Kshama Kulhali is a Head of the Department of Information Technology at D. Y. Patil Engineering College, Kolhapur, India. She earned her Ph.D. Degree from Shivaji University, Kolhapur, India and holds a M.Sc. Degree of Engineering from Birla Institute of Technology and Science, Pilani, India. Her research focuses on biomedical applications, artificial intelligence, image processing, mobile technology, and cryptography. Her work has been widely published in esteemed journals, conferences, and books. She also actively serves as a reviewer and is a member of several renowned journals and professional bodies in her field.

Assist. Prof. Priyanka Singh, Ph.D.
E-mail: priyanka.cse03@gmail.com

Dr. Priyanka Singh is a distinguished academic with a Ph.D. Degree in Computer Science and Engineering from National Institute of Technology, Silchar, India specializing in malware detection, machine learning, and deep neural networks. She holds an M.Sc. Technical Degree from Visvesvaraya Technological University, India and a B.Sc. Engineering Degree in Computer Science and Engineering from Solapur University, India. She has over nine years of teaching experience and currently is an Assist. Prof. at Vellore Institute of Technology, Andhra Pradesh, India. She has contributed significantly to research, publishing in esteemed international journals and conferences, particularly in malware detection and AI. Additionally, she organizes workshops and mentors students in cutting-edge areas of computer science.